Nanoscale

PAPER

View Article Online
View Journal | View Issue

Cite this: *Nanoscale*, 2019, **11**, 15270

Versatile route to core–shell reinforced network nanostructures†

Pascal Rusch,[a] Fabian Niemeyer,[a,c] Denis Pluta,[a,c] Björn Schremmer,[a] Franziska Lübkemann,[a] Marina Rosebrock,[a] Malte Schäfer,[b,c] Mandy Jahns,[b] Peter Behrens [b,c,d] and Nadja C. Bigall *[a,c,d]

Received 29th April 2019,
Accepted 19th July 2019

DOI: 10.1039/c9nr03645h

rsc.li/nanoscale

In this work we present the generation of new core–shell network nanostructures of macroscopic dimensionality by a two-step process analogous to the seeded-growth method in colloidal nanoparticle modification. The nanoparticle-based core network is assembled first and in a separate second step it is coated with a continuous metal oxide shell by sol–gel methods. The interparticle contact of the nanoparticles comprising the core network is kept intact throughout the process. By analyzing the local elemental distribution, the shells can be shown to be homogeneous over the macroscopic network monolith. The shell network can be used to considerably reinforce the mechanical strength of the final core–shell network structure.

Introduction

After the introduction of aerogels in 1931 by Kistler[1] and the optimistic outlook to extend the list of materials from which aerogels can be generated, it still took the better part of a century until a method was used to generate nanocrystal-based aerogel networks in 2005.[2,3] This method to form randomly oriented network structures out of pre-formed colloidal nanoparticles offers higher customizability as it allows the fine tuning of the individual building blocks by modern colloid chemical routes as opposed to the one-step generation of particles and networks in molecular routes of conventional sol–gel chemistry. In recent years the number of nanoparticle materials that were converted into such macroscopic and porous network structures steadily increased[4–7] and was expanded to noble metals[8] as well as a number of intricate particles provided by the well advanced chemical synthesis of nanoparticles.[9–13] The procedure usually includes the controlled destabilization of a colloidally stable nanoparticle solution, often by attacking the stabilizing ligand shell of the particle, *e.g.*, by oxidation agents. More recently different methods were described based on connecting the particles – sometimes also reversibly – *via* the interaction of ligands, organic and inorganic, with added cations.[14,15] Also methods completely free of chemical interactions but rather based on physical procedures have been employed.[16] Still, as the catalogue of new nanoparticles grows and the number of these converted into self-supporting 3D networks increases, generally this innovation stops once a network is indeed generated.

In this work we want to show that the network formation alone does not need to be the last step, but instead some of the modification procedures developed for colloidal nanoparticles can – under the right conditions – be applied to a nanoparticle network substrate as well. Network structures build up from metal nanoparticle building blocks have shown very promising results as catalysts in the oxygen evolution reaction[17,18] as well as fuel cell applications.[19] Similarly semiconductor nanoparticle based networks were employed as photocatalysts.[20] Our group recently demonstrated a semiconductor network based sensor also showing the higher sensitivity of the network compared to plain nanoparticles.[21] One drawback of the monolithic network structures is their poor mechanical stability which is widely regarded as the point inhibiting application of these networks.[22,23] Here, we propose the method of post-assembly shell growth as a new way to increase mechanical stability and thereby resolve one major problem holding self-supporting nanoparticle network structures back from their potential applications. For example, in recent studies of the catalytic activity of nanoparticle aerogels, it was found that either the networks had to be broken apart and dispersed[24] or the reaction conditions needed to be changed drastically[13] to accommodate this problem. It has recently been shown that it is possible to grow metallic shells

[a]*Institute of Physical Chemistry and Electrochemistry, Leibniz Universität Hannover, Callinstraße 3A, 30167 Hannover, Germany.*
E-mail: nadja.bigall@pci.uni-hannover.de
[b]*Institute for Inorganic Chemistry, Leibniz Universität Hannover, Callinstraße 9, 30167 Hannover, Germany*
[c]*Laboratory of Nano and Quantum Engineering, Leibniz Universität Hannover, Schneiderberg 39, 30167 Hannover, Germany*
[d]*Cluster of Excellency PhoenixD (Photonics, Optics, and Engineering – Innovation Across Disciplines), Hannover, Germany*

†Electronic supplementary information (ESI) available: Rehydration experiments, further TEM and SEM measurements. See DOI: 10.1039/c9nr03645h

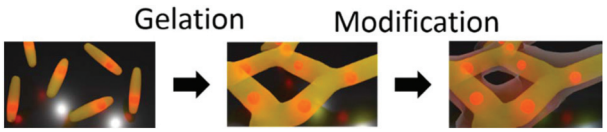

Fig. 1 Schematic depiction of the two-step process employed: first, the assembly of individual nanocrystal building blocks into a porous network structure and second the modification of this network by shell growth.

around nanoparticle-based networks by electrochemical deposition.[25] Our method also entails another modification step after the initial nanoparticle network formation but using wet-chemical methods. The method employed is similar to a seeded growth mechanism in colloid chemistry, where first nanocrystal seeds are synthesized and subsequently a different compound can be grown onto the seeds under conditions of heterogeneous nucleation only. In our method, however, instead of the seed nanoparticle we employ a seed nanoparticle network, as schematically shown in Fig. 1. More specifically, we propose the growth of metal oxide shells around the whole NANOparticle-based NETwork Structure (NANONETS) (consisting of interconnected nanocrystal building blocks) using sol–gel processes. The method presented in this work is applicable for different substrates as shown by the shell growth onto the semiconductor NANONETS as well as metallic ones. It can also be used to grow not only silica shells but also titania alike (also see Fig. 2). This indicates the versatility of our approach.

Contrary to other methods already published in the literature we do not embed particles in a gel matrix made of the metal oxide.[26–29] Instead the original network is made up of the nanoparticle based "core" network which is encased in a second "shell" network applying a post-assembly coating step. The crystal-to-crystal contact between the nanoparticles in the "core" network is still present in the newly formed structure, as schematically illustrated in Fig. 1.

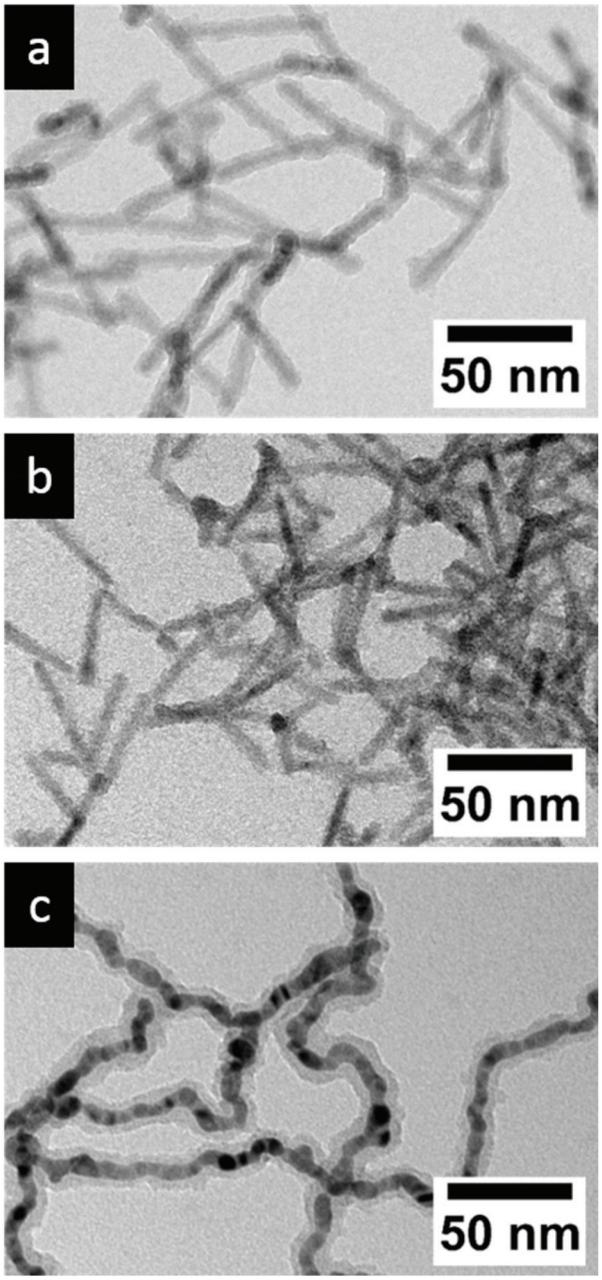

Fig. 2 Different material combination of post-gelation modified networks. (a) CdSe/CdS nanorod core network with a silica shell, (b) CdSe/CdS nanorod core network with a titania shell and (c) Au–Ag mixed core network with a silica shell.

Experimental

Chemicals used

Tri-*n*-octylphosphine oxide (TOPO, 99%), 3-mercaptopropionic acid (MPA, 99%), potassium hydroxide (KOH, >85%), hexane (99%), toluene (99.7%), methanol (99.8%), sulfur (S, 99.98%), ammonia (NH_3, 28.0–30.0% aqueous solution), titanium(IV) butoxide (97%), sodium borohydride (98%), (3-aminopropyl)-trimethoxysilane (APTMS, 97%) and tetraethyl orthosilicate (TEOS, 99.999%) were purchased from Sigma-Aldrich. Acetone (99.5%) and hydrogen peroxide (35% aqueous solution) were purchased from Honeywell. Cadmium oxide (CdO, 99.998%), hydrogen tetrachloroaurate trihydrate (99.99%), silver nitrate (99.9%) and selenium (Se, 99.999%) were purchased from Alfa Aesar. Hexylphosphonic acid (HPA, >99%) and octadecylphosphonic acid (ODPA, >99%) were purchased from PCI Synthesis. Tri-*n*-octylphosphine (TOP, 97%) and trisodium citrate dihydrate (99.0%) were purchased from ABCR. Acetylacetone (acac, 99%) was purchased from Merck. Ethanol (99.8%) was purchased from Roth. All chemicals were used as received.

Synthesis procedures

The CdSe/CdS nanorods used for network formation were synthesized according to the literature procedure[30] and assembled as described in earlier studies of our group.[12] The whole process will be described briefly here.

Synthesis of CdSe cores. CdSe quantum dots were synthesized by mixing 60 mg of CdO with 280 mg of ODPA and

3 g of TOPO in a 25 mL three-neck-flask and degassed at 150 °C for one hour. The temperature was raised to 300 °C under a nitrogen atmosphere to dissolve CdO. 1.8 mL of TOP was added and the mixture was heated to 380 °C. At this point 58 mg of Se powder dissolved in 1.8 mL of TOP (equimolar mixture) was injected by a syringe. Due to the injection the temperature of the mixture decreased, it was allowed to reach 380 °C again, and then the reaction mixture was cooled down to room temperature. The quantum dots were precipitated by the addition of methanol and centrifuged. The quantum dots were washed twice by dispersion in toluene and precipitation by methanol and afterwards stored in toluene.

Synthesis of CdSe/CdS nanorods by the seeded growth method. For the growth of rod shaped shells around the CdSe quantum dots 60 mg of CdO were mixed with 280 mg of ODPA, 80 mg of HPA, and 3 g of TOPO and degassed at 150 °C for one hour. Under a nitrogen atmosphere the temperature was increased to 300 °C and 1.8 mL of TOP is added. The temperature was raised to 380 °C and a mixture of S in TOP (130 mg S in 1.8 mL TOP) and the dissolved CdSe cores (400 μM, concentration estimated by optical spectroscopy[31]) was injected. After six minutes of reaction time the mixture was allowed to cool to room temperature. The nanorods produced by this method were precipitated, washed in a similar way to the quantum dots in the first step and stored in 6 mL of toluene.

Transfer of CdSe/CdS nanorods into aqueous solution. The phosphine capped nanorods need to be transferred into water for network formation. This was done by exchanging the ligands with mercaptopropionic acid (MPA) as described in the literature.[32,33]

The nanorods in solution (750 μL) were precipitated by the addition of methanol and centrifuged at 5000 rcf. The supernatant was discarded and the particles were dissolved in 10 mL of hexane. To this solution 242 μL of MPA was added as well as 10 mL of a 0.1 M solution of KOH in methanol. The mixture is shaken for 24 hours during which the now MPA capped nanorods precipitated. The particles were separated from the remaining phase transfer solution by centrifugation and could be dissolved in 0.1 M aqueous KOH.

Assembly of the CdSe/CdS nanorod network. The aqueous solution of nanorods was diluted to a cadmium ion concentration of 3.6 mg mL^{-1} and 800 μL of this solution were mixed with 75 μL of 0.35% hydrogen peroxide. The solution was thoroughly mixed and heated to 80 °C for one minute. It was then left undisturbed in the dark for one hour and afterwards a macroscopic network structure is formed. The network was washed by multiple additions of water and removal of the supernatant.

Synthesis of noble metal nanoparticle network structures. Noble metal nanoparticles were prepared and assembled into network structures according to literature procedures.[8] For the preparation of Au nanoparticles 36.2 mL of a 0.2 wt% $H[AuCl_4]\cdot 3H_2O$ solution was added to 465 mL of distilled water. To this solution 11.6 mL of 1% sodium citrate solution was added and after 30 seconds 5.5 mL of sodium borohydride solution (prepared by dissolving 39 mg of $NaBH_4$ in 50 mL of 1% sodium citrate solution) was quickly added. This was left to stir for 30 minutes. The prepared nanoparticle dispersion was concentrated by filtration down to a volume of 10 mL. During this the particles were washed by repeatedly adding 5 mL of distilled water and concentrated by filtration. Ag nanoparticles were prepared in a similar manner using 12 mL of 0.2% $AgNO_3$ solution as a noble metal precursor and by performing the reduction in boiling solution. The two noble metal nanoparticle dispersions were mixed in equal volumes (here 0.5 mL) and 0.4 mL of 1% hydrogen peroxide solution was added to the mixture. Network formation took place within 5 weeks.

Modification of networks with a metal oxide shell. As the first step of modification of the nanoparticle network with a silica shell the solvent surrounding the network had to be thoroughly exchanged to methanol as residual water will influence the formation of silica. The solvent exchange was done by discarding the liquid above the network and adding fresh methanol. This process was repeated twice a day for at least five days. Afterwards tetraethyl orthosilicate (TEOS) as a silica precursor was added and the sample was left undisturbed for 24 hours to give the precursor time to diffuse into the network pores. The amount of TEOS used is calculated in relation to the cadmium amount inside the network. A typical network contained 2.88 mg or 26 μmol of cadmium. For an equimolar relation of cadmium and silicon, 5.7 μL of TEOS was needed. After the one-day period a specific amount of water (0–50 mmol) and ammonia (0–400 μmol) was added to the sample and it was again left undisturbed for 24 hours to react. After the reaction the network structure was washed with methanol by repeatedly exchanging the solvent to fresh methanol to flush out byproducts.

The coating of networks with titania was performed accordingly using titanium *n*-butoxide as a metal oxide precursor. As the hydrolysation of titanium alkoxides is much faster than the reaction of the equivalent silicon compounds acetylacetonate was added in this case to slow down the reaction by complexing the titanium cation. The amount of acetylacetonate was chosen in relation to the amount of titania precursor added.

The coating of noble metal nanoparticle based networks was performed in an identical manner. In this case the addition of a linker, namely, APTMS, at a 0.1 ratio compared to the noble metal concentration could be used to improve the uniformity of the shells.

Supercritical drying. To dry the nanoparticle network, structures were transferred into dry acetone by exchanging the solvent twice per day for at least five days with acetone dried over molecular sieves, 3 Å. The samples prepared by this solvent exchange were carefully loaded into a critical point dryer (Quorum Technologies E3100). The apparatus was filled and additionally flushed for five minutes with liquid CO_2 at a pressure of 55 bar at 20 °C. CO_2 was allowed to diffuse into the network overnight and flushing was repeated once before drying. For supercritical drying the drier was heated above the critical point of CO_2 at 31.1 °C. During the process the pressure inside the drying chamber rose to about 73 bar. Once

CO_2 was in the supercritical state it was allowed to slowly vent into the atmosphere while retaining temperatures above 31 °C. Once the pressure inside the drying chamber was at the atmospheric value the dried networks could be recovered from the apparatus and were further characterized.

Characterization

Electron microscopy. TEM samples of nanoparticles in solution were prepared by drop casting diluted solutions in chloroform onto a carbon coated copper grid (300 mesh) by Quantifoil. For sample preparation of dried networks, the mentioned grids were pulled along the sample, thereby keeping small parts of the network stuck to the grid. The bright-field (BF-TEM) measurements were carried out using a FEI Tecnai G2 F20 transmission electron microscope with a field emission gun operating at 200 kV. For high-angle annular dark field (HAADF-STEM) measurements coupled with energy-dispersive X-ray spectroscopy (EDX) a JEOL JEM-2100F with an acceleration voltage of 200 kV was employed.

SEM samples were prepared by finely slicing off a part of the macroscopic network structure with a scalpel. This section was stuck to the adhesive carbon film and measured. The SEM used was a JEOL JSM 6700F field emission scanning electron microscope with an acceleration voltage of 2 kV and a secondary electron detector at a working distance of 8 mm. In the SEM, elemental analysis was performed using an Oxford Instruments INCA 300 energy dispersive X-ray spectrometer with the SEM operating at 10 kV at a working distance of 15 mm.

Compression tests. The compression tests were performed on an Instron 5565A by placing the monolithic dried network structure between the plates of the device. As the samples are not completely uniform, an irregular shape was assumed for the interpretation of the data. The contact area between the pressure plate and the sample was estimated by measuring the area of the sample from a photograph taken from above. The plates are pressed together at a constant rate of 0.2 mm s^{-1} and the force acting on the plates is measured. The measurement was stopped when either the material showed a mechanical failure (in the case of the unmodified gel in the form of multiple breakages) or when the pressure reached 50 N. The stress and strain are calculated using the initial contact area of the monolith and plate and the initial height of the monolith, respectively.

Physisorption measurements. Physisorption measurements were carried out on a Quantachrome Autosorb-1 at 87 K employing Krypton as the measurement gas. Before the measurement the samples were degassed at room temperature for 24 h. The surface areas were estimated using the Brunauer–Emmett–Teller (BET) equation.[34]

Results and discussion

For the functionalization of nanoparticles with a silica shell, a plethora of methods is described in the literature which are mostly based on the Stöber process.[35] Due to the substrate not being a nanoparticle in solution but rather a macroscopic body (consisting of a network of nanocrystals), methods involving microemulsions[36,37] could not be used. We therefore opted for a synthesis that is similar to the direct coating methods reported,[38,39] with much simpler conditions than the microemulsion routes in terms of the solvent system since no surfactants are employed, see the Experimental section for details. This procedure could be used with small adaptions for the growth of titania shells as well as for the growth of silica on noble metal NANONETSs. The successful modification of the NANONETS with a metal oxide shell can be observed by transmission electron microscopy (TEM) as shown in Fig. 2.

For the pristine semiconductor NANONETS a smooth surface of the NRs forming the network is visible (Fig. 3b) in the TEM measurements. With increasing amounts of metal oxide precursor added to the structure there is no optical difference between the dried network structures as can be seen in the photographs under UV- and daylight (Fig. 3a). In electron microscopy an increase in surface roughness is visible due to small domains of silica forming on the nanocrystal surfaces (see Fig. 3c and d). In these cases, the difference in electronic TEM contrast between silica and the NRs is unfortunately not sufficient to make the new shell clearly distinguishable from cadmium sulfide. With higher amounts of silica precursor and consequently thicker shells, the core network and the surrounding silica shell become easily discernable (Fig. 3e). The porous structure of the network is visible in the SEM (Fig. 4d) and could also be measured by krypton physisorption. The surface area derived from the BET evaluation is 100 m^2 g^{-1} for the unmodified network which is comparable to the ones reported for similar structures.[11,40] After the modification the BET surface areas increase considerably to 160–180 m^2 g^{-1} potentially due to microporosity in the silica shell itself as well as the higher mechanical stability, preventing the network from damage during processing. It also indicates that the modification does not block the porosity of the network (see Fig. S11†).

The successful modification with a homogeneous silica shell is clearly visible in the nanometer size regime. However, this only shows the modification in a random spot test. Hence, to investigate the homogeneity of the modification on a much larger scale, scanning electron microscopy (SEM) with elemental analysis by energy-dispersive X-ray spectroscopy (EDX) is employed. The elemental distribution is measured at different positions of a section of the modified NANONETS. These samples are prepared by slicing a thin piece off the body of the network structure (possible for samples with Si/Cd ratios larger than 1) without further modification of the sample (schematically shown in Fig. 4a). It should be noted that this is to the best of our knowledge the first time that the dried network of nanoparticles can be cut easily by simply employing a scalpel, since "conventional" nanocrystal network structures are either far too brittle or far too deformable for such a preparation method. By our post-assembly silica growth route, it is possible to perform structural investigations of nanocrystal network structures to a greater extent. Here, we have investigated the ratio of Si/Cd at various points in the NANONETS (center, top, bottom, and outer areas) in order to determine

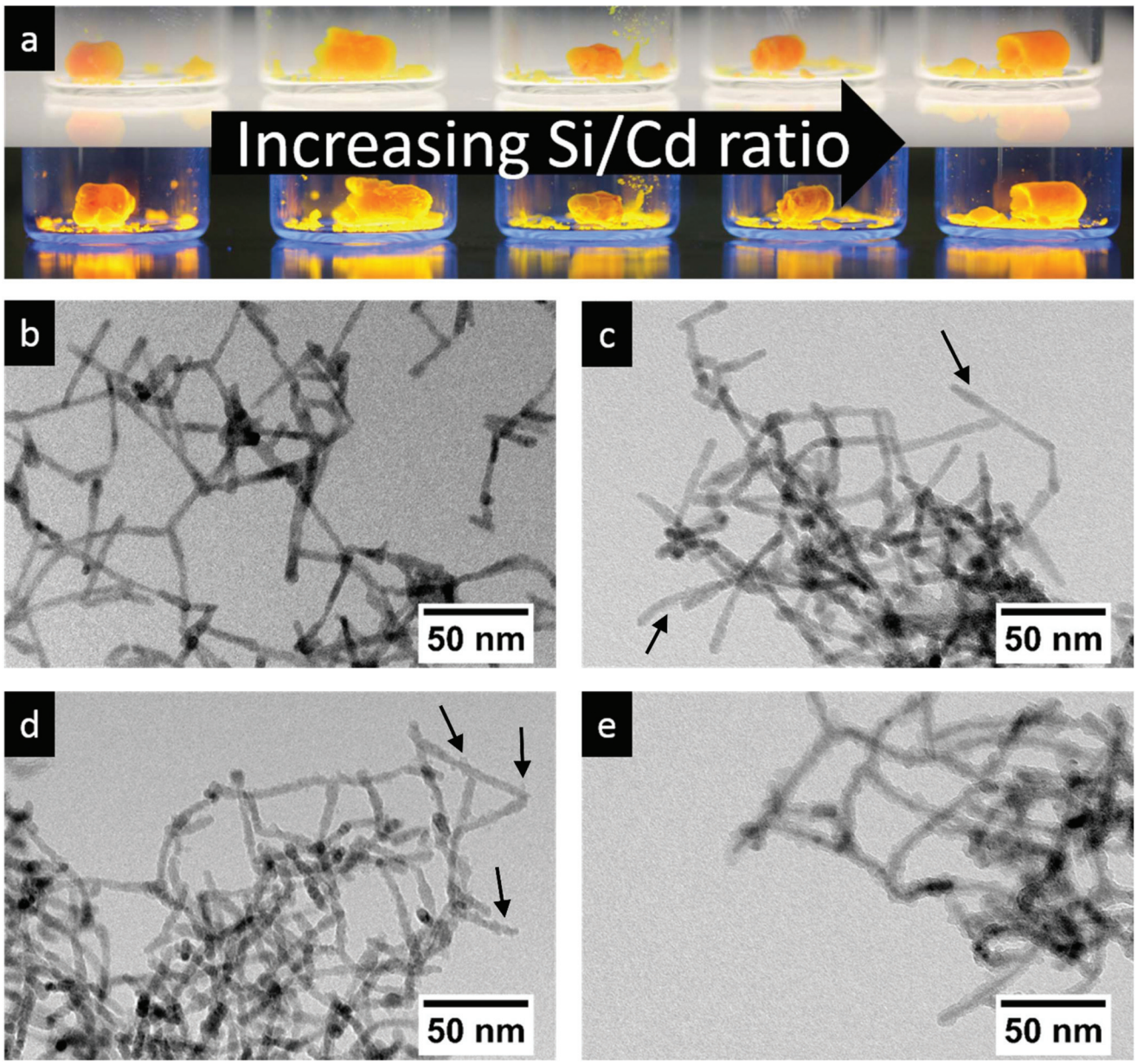

Fig. 3 Core–shell network structures prepared with different ratios of silica precursors relative to the cadmium content of the core network. (a) Photographs of the monolithic dried networks under ambient (top) and UV (bottom) light with increasing amounts of silica precursor added from left to right (starting at 0 to 10/1). TEM micrographs of networks modified with different silica/cadmium ratios, (b) 0/1, (c) 1/1, (d) 2/1 and (e) 10/1. Arrows are used to indicate some of the recognizable domains of silica growth on the building block surfaces.

the homogeneity of our silica shell growth route. The SEM images show the highly porous network structure expected for these types of nanoparticle assemblies (Fig. 4d). The elemental measurements illustrate the silica-shell modification as well as its homogeneity. In the case of low silica amounts (Si/Cd < 1/1) the NANONETS breaks uncontrollably during sample preparation and random measurement positions were chosen (see the ESI†). Still, the elemental measurements fit well within our assumption of a largely homogeneous silica shell growth as discussed in the ESI.† For higher amounts of silica the NANONETS can be sliced in a controlled way and so the elemental distribution can be examined from the surface of the NANONETS down to the center. As an example, the measurement positions for one sample are marked in Fig. 3c on an overview (for positions on other samples see Fig. S4–S6† for the corresponding EDX spectra). In the case of NANONETSs modified with an initial (that is, as inserted during synthesis) ratio of 2/1 of Si/Cd, this initial ratio is retained for the surface part of the final structure, while in the center the ratio drops to 1.64/1. When an initial ratio of 10/1 of Si/Cd is used, the ratio measured from the surface of the NANONETS is 7.5/1 (measured at the position "outside") going down to 4.8/1 inside the structure (measured at the position "center"). This gradient in the Si/Cd ratio exemplifies the strong influence of

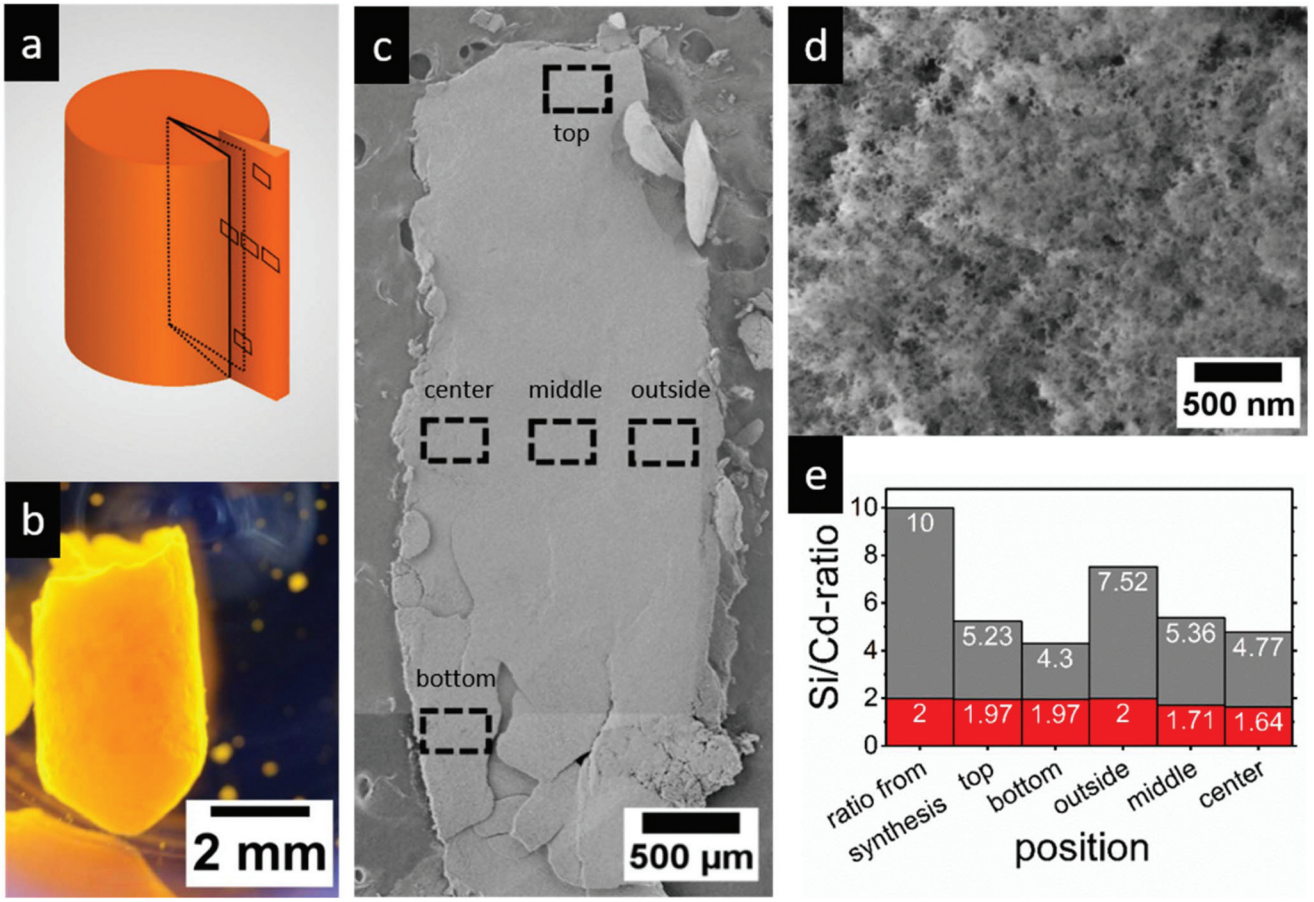

Fig. 4 Analysis of local elemental distribution to evaluate the homogeneity of the silica shells. (a) Schematic depiction of the SEM sample in relation to the whole network body and (b) photograph of a dried network monolith under UV light to demonstrate the shape analogy. (c) Large scale SEM micrograph of the network slice modified with an initial Si/Cd ratio of 10/1, depicting the measurement positions for EDX (assembled from two separate pictures) and (d) higher resolution SEM image of the same network structure displaying the porous structure. (e) Si/Cd ratio found by EDX measurements at various measurement positions for initial Si/Cd ratios of 10/1 in grey and 2/1 in red.

the transport limitation inside of the network pores, so that the modification is therefore not totally uniform for the whole of the macroscopic body of the NANONETS. On the other hand, it also shows that the modification is – while not completely uniform – present over the whole macroscopic network. It needs to be taken into account that transport is a major obstacle in the attempt of transferring nanoparticle modification methods in colloidal solution onto nanoparticle network substrates. Considering that the size regime of the distance that the silica precursors have to travel is increased from nanometers in a colloid to millimeters in such types of networks, the silica shells produced by this method throughout the structure are remarkably homogeneous.

The pH-value and concentration of water are key parameters for the Stöber synthesis. The standard parameters for this work have been adapted from literature procedures for the functionalization of noble metal nanoparticles with a silica shell in solution.[41] The parameters are then varied to optimize the functionalization for a NANONETS substrate. The amount of water and ammonia is varied from no addition of the reactant to a tenfold excess in the case of ammonia or a fivefold excess in the case of water compared to the standard values adapted from the literature. All other parameters are kept constant. From the TEM micrographs of the NANONETS the clear necessity of both water and ammonia for the modification process can be derived. If neither water nor ammonia is added (Fig. S2a†) the shell growth is highly inhomogeneous even on a low size scale. Silica forms probably by reaction with residual water in the pores or from the atmosphere, but it does not form a clearly defined shell around the network. Instead some pores are filled with silica, while no silica is visible in other places. If only 30% ammonia solution is added but no additional water, the results are quite similar (Fig. S2b†). In this case a silica gel seems to form encasing the original NANONETS. The pores of the original structure are filled with the silica material. If water is added but no ammonia, the growth of silica also appears to be largely inhomogeneous (Fig. S3a†) with thicker silica shells visible at certain spots and no shell visible at other places. As soon as both reactants, water and ammonia, are added, the desired structure of the original NANONETS is surrounded by a continuous silica shell without any visible side nucleation. While the amount of

ammonia does not seem to have a pronounced influence for the volumes investigated as long as it is present (Fig. S3†), water concentrations between 2 and 10 mmol mL^{-1} yield the most homogeneous and pronounced silica shells (Fig. S2†).

It was also investigated if it was possible to transfer these reaction conditions while changing either the core network material or the shell material. To this end similar conditions were applied while using titanium butoxide instead of tetraethyl orthosilicate (Fig. 1c). With this it was possible to grow titania shells in an equal manner (also see Fig. S7†). Slight adjustments in this procedure are needed such as the addition of acetylacetone (acac). acac acts as a chelating ligand which considerably decreases the reactivity of the precursor. This counteracts the effect that titania alkoxides are in general much more reactive compared to silica alkoxides as has been described for similar processes in colloidal particle modification (also see Fig. S8†).[42,43] When examining the local elemental distribution by SEM-EDX as described for the silica shells earlier this influence is clearly visible. Without the addition of acac the homogeneous nucleation of titania outside of the network is immediately visible even by the eye. If the amount of acac in relation to the amount of titania precursor is increased the ratio of Ti/Cd measured inside the network increases due to the suppression of homogeneous nucleation. Also the homogeneity increases, indicated by the small difference in the Ti/Cd ratio measured at different spots on the gel. However, if very high amounts of acac are added the titania shell formation inside the gel is suppressed and there is almost no titania grown in this instance. A ratio of 2/1 acac/Ti-precursor seems to yield the most promising results in this study. The BET surface area of this titania modified network is *ca.* 140 $m^2\ g^{-1}$ which is still higher than that of the unmodified networks (see Fig. S11†).

Furthermore, it was possible to use networks assembled from a mixture of gold and silver nanoparticles to grow a noble metal core silica shell network. Electron micrograms of these are shown in Fig. 5. The nanoparticles assemble into a chain-like interconnected highly porous network structure. In higher magnifications the silica shell is clearly visible homogeneously surrounding the whole continuous network (Fig. 5b). Measuring the elemental distribution at high magnifications is very difficult as the networks tend to move during the measurement. Still in the HAADF-STEM the shell is visible as a slightly brighter shell surrounding the noble metal chains. In the EDX signals of all three elements of interest (Au, Ag and Si) are detected along the chains of the network (Fig. 5c and d). The physisorption measurements revealed a BET surface area of the pristine Au–Ag nanoparticle networks of 25 $m^2\ g^{-1}$ which is similar to the values reported in the literature.[8] As was the case for semiconductor nanoparticle based networks this surface area increases considerably with the silica modification to 105 $m^2\ g^{-1}$ (see Fig. S11†). This hints at the large inner surface of the porous silica shell. Similar to the growth of titania shells in this instance it was also needed to minimally adjust the experimental procedure. The addition of low amounts of a silica linker (here: 3-aminopropyl-trimethoxysilane, at a 0.1 ratio compared to the amount of silica precursor used) was needed to grow homogeneous shells (also see Fig. S9† for details). Without the addition of a linker the shell growth is not homogeneous and limited to randomly dispersed spots on the network structure.

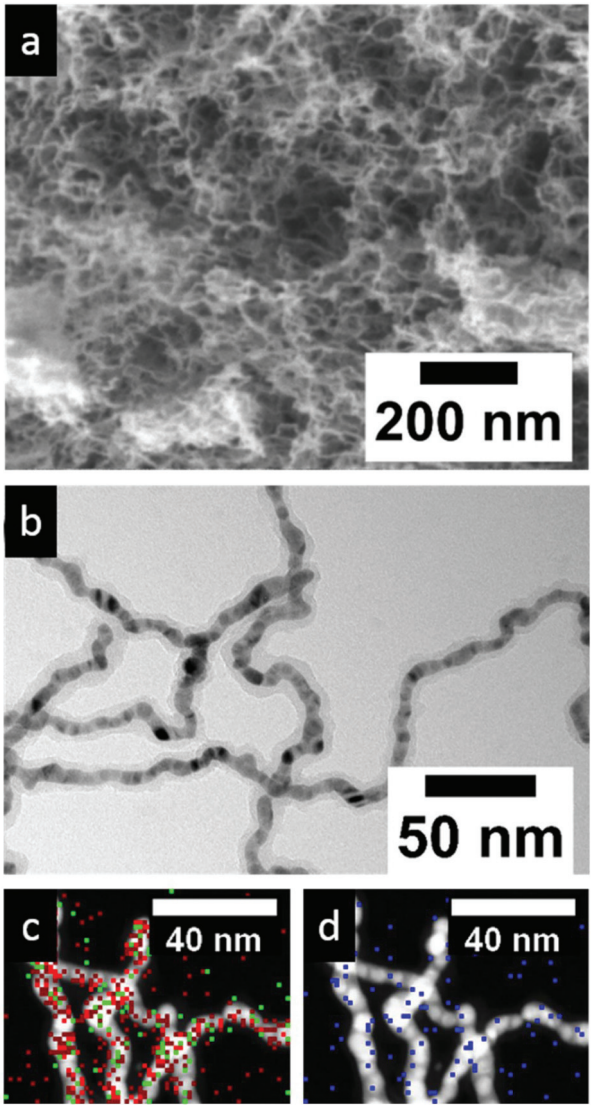

Fig. 5 Network consisting of a mixture of Au and Ag nanoparticles with a silica shell grown around the network in (a) SEM, (b) BF-TEM and (c, d) HAADF-STEM with the overlaying EDX measurement. Red color indicates Au, green Ag and blue Si.

The silica shell modification was expected to considerably increase the resistivity of the NANONETS towards mechanical stress as the network is essentially reinforced by the shell. Although the mechanical instability of nanoparticle networks is often a drawback it is seldom investigated or even mentioned in the literature. In fact the studies of mechanical properties have been reported only for organic aerogels,[44,45] carbon aerogels[46,47] or silica aerogels[48,49] and recently for other metal–oxide aerogels.[50] In this work a compression test was employed to evaluate the mechanical stability of silica

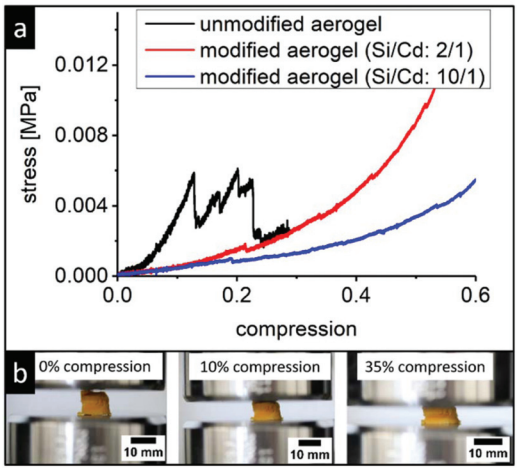

Fig. 6 (a) Mechanical measurement of dried silica shell modified and unmodified CdSe/CdS NR networks by compression tests. The photographs (b) show a silica shell modified network structure (Si/Cd 10/1) at various points of the measurement.

shell modified and unmodified NANONETSs. As the dimensions of the NANONETS are small, and as the forces the samples are subjected to are also very small, it is not possible to actually measure the Young's modulus (which is usually done in the area of elastic deformation at low strain levels). Still, information about the relative mechanical stability can be obtained by the measurements performed. The measurements of the unmodified NANONETS show a drastic drop in stress, which occurs when a large part of the structure breaks and is a signature of its brittleness.

This is not observed in the case of silica modified networks (see Fig. 6) within the measurement range investigated. In a more practical context this increased mechanical resistance can also be observed when the dried NANONETS is added back to a solvent, *i.e.*, water. The unmodified NANONETS falls apart in a few seconds into a multitude of small particles (Fig. S10†), which we attribute to the occurrence of capillary forces. In contrast, the silica shell modified NANONETS sinks to the bottom of the container after some time while still remaining largely in one piece (also see Fig. S10†). This result further emphasizes the benefit of post-assembly silica shell growth for nanoparticle aerogels, since it enables rehydration while keeping the advantageous properties of the nanocrystal networks in the macroscopic body.

Conclusions

In summary, we have presented a novel approach to the metal oxide shell modification of the NANONETS which leaves the initial network and the interparticle crystal-to-crystal contact intact. To our knowledge this marks the first time that the possibility of modifying self-supporting nanocrystal networks by a sol–gel post-assembly modification with a thin inorganic shell has been described. This process leads to a new, formerly unknown structure. This method was employed to successfully coat nanostructures of different compositions ranging from the semiconducting to metallic ones and is therefore highly versatile. It could also be expanded to the growth of titania instead of silica. The integrity of the nanocrystal network could be confirmed by electron microscopy measurements and the homogeneity of the silica shell was examined by local elemental analysis and found to be highly uniform over the whole body for all modifications performed. It could be shown that the modification with silica shells severely increases the mechanical stability of the structures, which can now be cut into pieces without breaking. All of this opens up a plethora of new possible applications of nanocrystal network assemblies in, *e.g.*, electrochemistry or catalysis where the network structures would need to be rehydrated with an electrolyte while maintaining the network properties. Due to the increased mechanical stability the fabrication of flow-through reactors can be imagined as well as the introduction of external stirring to facilitate mixing. All this can be done while retaining the monolithic structure, leading to an easy separation. As the particles forming the core network are still connected the networks should be able to conduct generated charge carriers, potentially improving the efficiency of the catalyst. Also the transfer of this method to other catalytically active metal oxides could prove interesting.

Conflicts of interest

There are no conflicts to declare.

Acknowledgements

The authors would like to thank Armin Feldhoff and Juergen Caro for the use of the SEM, as well as the Laboratory of Nano and Quantum Engineering for the use of the TEM and their support. The authors would also like to thank the REBIRTH cluster of excellence for access to the mechanical testing experiment. The project leading to these results received funding from the European Research Council (ERC) under the European Union's Horizon 2020 research and innovation programme (grant agreement No. 714429). N. C. B. furthermore acknowledges funding from German Federal Ministry of Education and Research (BMBF) within the framework of NanoMatFutur (support code 03X5525). This project was in part funded by the Deutsche Forschungsgemeinschaft (DFG, German Research Foundation) under Germany's Excellence Strategy within the Cluster of Excellence PhoenixD (EXC 2122). M. S. is grateful for a fellowship from the PhD programme "Hannover School for Nanotechnology-Sensors" of the LNQE, funded by the state of lower Saxony.

Notes and references

1 S. S. Kistler, *Nature*, 1931, **127**, 741–741.
2 J. L. Mohanan, I. U. Arachchige and S. L. Brock, *Science*, 2005, **307**, 397–400.

3 I. U. Arachchige, J. L. Mohanan and S. L. Brock, *Chem. Mater.*, 2005, **17**, 6644–6650.
4 K. K. Kalebaila, D. G. Georgiev and S. L. Brock, *J. Non-Cryst. Solids*, 2006, **352**, 232–240.
5 A. Hitihami-Mudiyanselage, K. Senevirathne and S. L. Brock, *ACS Nano*, 2013, **7**, 1163–1170.
6 S. Ganguly and S. L. Brock, *J. Mater. Chem.*, 2011, **21**, 8800.
7 N. Gaponik, A. Wolf, R. Marx, V. Lesnyak, K. Schilling and A. Eychmüller, *Adv. Mater.*, 2008, **20**, 4257–4262.
8 N. C. Bigall, A.-K. Herrmann, M. Vogel, M. Rose, P. Simon, W. Carrillo-Cabrera, D. Dorfs, S. Kaskel, N. Gaponik and A. Eychmüller, *Angew. Chem., Int. Ed.*, 2009, **48**, 9731–9734.
9 H. Yu and S. L. Brock, *ACS Nano*, 2008, **2**, 1563–1570.
10 I. U. Arachchige and S. L. Brock, *J. Am. Chem. Soc.*, 2007, **129**, 1840–1841.
11 S. Naskar, J. F. Miethe, S. Sanchez-Paradinas, N. Schmidt, K. Kanthasamy, P. Behrens, H. Pfnür and N. C. Bigall, *Chem. Mater.*, 2016, **28**, 2089–2099.
12 S. Sanchez-Paradinas, D. Dorfs, S. Friebe, A. Freytag, A. Wolf and N. C. Bigall, *Adv. Mater.*, 2015, **27**, 6152–6156.
13 S. Naskar, A. Freytag, J. Deutsch, N. Wendt, P. Behrens, A. Köckritz and N. C. Bigall, *Chem. Mater.*, 2017, **29**, 9208–9217.
14 V. Lesnyak, S. V. Voitekhovich, P. N. Gaponik, N. Gaponik and A. Eychmüller, *ACS Nano*, 2010, **4**, 4090–4096.
15 V. Sayevich, B. Cai, A. Benad, D. Haubold, L. Sonntag, N. Gaponik, V. Lesnyak and A. Eychmüller, *Angew. Chem., Int. Ed.*, 2016, **55**, 6334–6338.
16 A. Freytag, S. Sánchez-Paradinas, S. Naskar, N. Wendt, M. Colombo, G. Pugliese, J. Poppe, C. Demirci, I. Kretschmer, D. W. Bahnemann, P. Behrens and N. C. Bigall, *Angew. Chem., Int. Ed.*, 2016, **55**, 1200–1203.
17 W. Liu, A.-K. Herrmann, D. Geiger, L. Borchardt, F. Simon, S. Kaskel, N. Gaponik and A. Eychmüller, *Angew. Chem., Int. Ed.*, 2012, **51**, 5743–5747.
18 W. Liu, P. Rodriguez, L. Borchardt, A. Foelske, J. Yuan, A.-K. Herrmann, D. Geiger, Z. Zheng, S. Kaskel, N. Gaponik, R. Kötz, T. J. Schmidt and A. Eychmüller, *Angew. Chem., Int. Ed.*, 2013, **52**, 9849–9852.
19 S. Henning, H. Ishikawa, L. Kühn, J. Herranz, E. Müller, A. Eychmüller and T. J. Schmidt, *Angew. Chem., Int. Ed.*, 2017, **56**, 10707–10710.
20 L. Korala, J. R. Germain, E. Chen, I. R. Pala, D. Li and S. L. Brock, *Inorg. Chem. Front.*, 2017, **4**, 1451–1457.
21 A. Schlosser, L. C. Meyer, F. Lübkemann, J. F. Miethe and N. C. Bigall, *Phys. Chem. Chem. Phys.*, 2019, **21**, 9002–9012.
22 B. Cai, V. Sayevich, N. Gaponik and A. Eychmüller, *Adv. Mater.*, 2018, **30**, 1707518.
23 W. Wan, R. Zhang, M. Ma and Y. Zhou, *J. Mater. Chem. A*, 2018, **6**, 754–775.
24 D. Wen, W. Liu, D. Haubold, C. Zhu, M. Oschatz, M. Holzschuh, A. Wolf, F. Simon, S. Kaskel and A. Eychmüller, *ACS Nano*, 2016, **10**, 2559–2567.
25 B. Cai, R. Hübner, K. Sasaki, Y. Zhang, D. Su, C. Ziegler, M. B. Vukmirovic, B. Rellinghaus, R. R. Adzic and A. Eychmüller, *Angew. Chem., Int. Ed.*, 2018, **57**, 2963–2966.
26 S. Jun, J. Lee and E. Jang, *ACS Nano*, 2013, **7**, 1472–1477.
27 Z. Li, L. Kong, S. Huang and L. Li, *Angew. Chem., Int. Ed.*, 2017, **56**, 8134–8138.
28 B. Belache, Y. Khelfaoui, M. Bououdina, T. Souier and W. Cai, *Mater. Sci. Semicond. Process.*, 2018, **76**, 42–49.
29 L. G. Tartuci, L. F. T. Domingos, J. Bettini, K. O. Vieira, E. Raphael, B. R. C. Vale, J. L. Ferrari and M. A. Schiavon, *J. Nanopart. Res.*, 2017, **19**, 250.
30 L. Carbone, C. Nobile, M. De Giorgi, F. Della Sala, G. Morello, P. Pompa, M. Hytch, E. Snoeck, A. Fiore, I. R. Franchini, M. Nadasan, A. F. Silvestre, L. Chiodo, S. Kudera, R. Cingolani, R. Krahne and L. Manna, *Nano Lett.*, 2007, **7**, 2942–2950.
31 W. W. Yu, L. Qu, W. Guo and X. Peng, *Chem. Mater.*, 2003, **15**, 2854–2860.
32 T. Kodanek, H. M. Banbela, S. Naskar, P. Adel, N. C. Bigall and D. Dorfs, *Nanoscale*, 2015, **7**, 19300–19309.
33 H. G. Bagaria, E. T. Ada, M. Shamsuzzoha, D. E. Nikles and D. T. Johnson, *Langmuir*, 2006, **22**, 7732–7737.
34 S. Brunauer, P. H. Emmett and E. Teller, *J. Am. Chem. Soc.*, 1938, **60**, 309–319.
35 W. Stöber, A. Fink and E. Bohn, *J. Colloid Interface Sci.*, 1968, **26**, 62–69.
36 X. Tang, E. Kröger, A. Nielsen, C. Strelow, A. Mews and T. Kipp, *Langmuir*, 2017, **33**, 5253–5260.
37 F. Pietra, R. J. A. van Dijk - Moes, X. Ke, S. Bals, G. Van Tendeloo, C. de Mello Donega and D. Vanmaekelbergh, *Chem. Mater.*, 2013, **25**, 3427–3434.
38 E. Mine, A. Yamada, Y. Kobayashi, M. Konno and L. M. Liz-Marzán, *J. Colloid Interface Sci.*, 2003, **264**, 385–390.
39 Y. Kobayashi, H. Katakami, E. Mine, D. Nagao, M. Konno and L. M. Liz-Marzán, *J. Colloid Interface Sci.*, 2005, **283**, 392–396.
40 H. Yu and S. L. Brock, *ACS Nano*, 2008, **2**, 1563–1570.
41 E. Mine, A. Yamada, Y. Kobayashi, M. Konno and L. M. Liz-Marzán, *J. Colloid Interface Sci.*, 2003, **264**, 385–390.
42 S. Lee, K. Lee, W. D. Kim, S. Lee, D. J. Shin and D. C. Lee, *J. Phys. Chem. C*, 2014, **118**, 23627–23634.
43 X. Zhang, H. Sun, X. Tao and X. Zhou, *RSC Adv.*, 2014, **4**, 31313–31317.
44 K. Kanamori, M. Aizawa, K. Nakanishi and T. Hanada, *Adv. Mater.*, 2007, **19**, 1589–1593.
45 H. Sehaqui, M. Salajková, Q. Zhou and L. A. Berglund, *Soft Matter*, 2010, **6**, 1824.
46 C. Zhu, T. Y.-J. Han, E. B. Duoss, A. M. Golobic, J. D. Kuntz, C. M. Spadaccini and M. A. Worsley, *Nat. Commun.*, 2015, **6**, 6962.
47 H.-W. Liang, Q.-F. Guan, L.-F. Chen, Z. Zhu, W.-J. Zhang and S.-H. Yu, *Angew. Chem., Int. Ed.*, 2012, **51**, 5101–5105.
48 J. P. Randall, M. A. B. Meador and S. C. Jana, *ACS Appl. Mater. Interfaces*, 2011, **3**, 613–626.
49 K. E. Parmenter and F. Milstein, *J. Non-Cryst. Solids*, 1998, **223**, 179–189.
50 A. Benad, F. Jürries, B. Vetter, B. Klemmed, R. Hübner, C. Leyens and A. Eychmüller, *Chem. Mater.*, 2018, **30**, 145–152.